

# Astrophysical Properties of the Sirius Binary System Modeled with MESA\*

MOMIN Y. KHAN<sup>1</sup> AND BARBARA G. CASTANHEIRA<sup>1</sup>

<sup>1</sup>*Department of Physics, Baylor University, Waco, TX 76798-7316*

## ABSTRACT

Sirius is the brightest star in the night sky and, despite its proximity, this binary system still imposes intriguing questions about its current characteristics and past evolution. [Bond et al. \(2017\)](#) published decades of astrometric measurements of the Sirius system, determining the dynamical masses for Sirius A and B, and the orbital period. We have used these determinations, combined with photometric determinations for luminosity and spectroscopic determinations of effective temperature ( $T_{\text{eff}}$ ) and metallicity, to model the evolution of the Sirius system using MESA (Modules for Experiments in Stellar Astrophysics). We have constructed a model grid calculated especially for this system and were able to obtain, for Sirius B, a progenitor mass of  $6.0 \pm 0.6 M_{\odot}$ , yielding a white dwarf mass of  $1.015 \pm 0.189 M_{\odot}$ . Our best determination for age of the system is  $203.6 \pm 45$  Myr with a metallicity of 0.0124. We have compared our best fit models with the ones computed using TYCHO, YREC, and PARSEC, establishing external uncertainties. Our results are consistent with the observations and support a non-interacting past.

*Keywords:* Stellar ages(1581) – Stellar evolution(1599) – Stellar mass functions(1612) – Visual binary stars(1777)

## 1. INTRODUCTION

The Sirius binary system is one of the closest binaries to Earth at only  $2.64 \pm 0.01$  pc ([van Leeuwen 2007](#)). Early observations of the astrometric perturbations of Sirius A led to the discovery of an unseen companion ([Bessel 1844](#)), which would become the prototype of the white dwarf stars, Sirius B. [Adams \(1915\)](#) first noted the similarities of the spectra of Sirius A and B despite the different values for masses and luminosities of these stars. Sirius B and subsequent stars with similar characteristics were called white dwarfs ([Luyten 1922](#)), and studied as a class by [Russell \(1944\)](#). The vast majority of white dwarfs are observed to be single stars, but studies of the Solar neighborhood indicated that approximately 8% are members of “Sirius-like” systems ([Holberg et al. 2013](#)), with at least one component of spectral type K or earlier.

The initial-to-final mass relation (IFMR) of stars is fundamental in the overall understanding of stellar evolution, from the star formation history to the stellar

populations and the interpretation of stellar luminosity distributions. To determine the IFMR, studies of stellar populations estimated empirically this relationship, using star clusters [e.g. [Cummings et al. \(2018\)](#) and references within]. “Sirius-like” systems are very useful to the study of IFMR, as well as of the white dwarf mass–radius relationship.

Over the past few decades, much effort has been put into modeling the evolution of Sirius A and B ([Liebert et al. 2005](#)), but fitting the observed parameters of the brightest star in the sky and its companion remains a challenging exercise.

[Bond et al. \(2017\)](#) published a historic analysis of decades of astrometric data using the Hubble Space Telescope, photographic observations, and measurements dating back to the 19<sup>th</sup> century to determine the dynamical masses and orbital properties of the Sirius system. We have used their mass measurements of  $2.063 \pm 0.023 M_{\odot}$  and  $1.018 \pm 0.011 M_{\odot}$  for Sirius A and B, respectively, and the orbital period of 50.13 years of Sirius B, with an eccentricity of 0.59, and additional determinations of effective temperature ( $T_{\text{eff}}$ ) and metallicity to probe its evolution. We computed a model grid for the Sirius system, using the Modules for Experiments in Stellar Astrophysics (MESA), an open-source 1D stel-

[momin.khan1@baylor.edu](mailto:momin.khan1@baylor.edu)

\* Released on March, 1st, 2021

lar evolution code (Paxton et al. 2011, 2013, 2015, 2018, 2019; Jermyn et al. 2023).

In this paper, we present the parameter space of the model grid calculated for the stellar evolution of the Sirius system and our best model. We then compared our results with the ones from previous studies, establishing external uncertainties in our determinations. Our goal is not only to provide a better understanding of the evolution of Sirius A and B, but also to shed light on modeling the evolution of binary systems as a whole.

## 2. OBSERVATIONAL PARAMETERS

In this section, we discuss the observed physical quantities to determine the parameter space of our model grid for the Sirius system. We have made our choices based on how well constrained they are, discussing the internal and external uncertainties, and model dependency.

### 2.1. Astrometric Measurements

When stars are members of binary systems, astrometric measurements provide the most precise mass determinations; it is equivalent of putting the stars on a balance scale. Because of the intrinsically robust nature of the astrometric determinations, we have fixed the values of mass of Sirius A, determined by Bond et al. (2017), as  $2.063 \pm 0.023 M_{\odot}$ . The current mass of Sirius B,  $1.018 \pm 0.011 M_{\odot}$ , also determined by Bond et al. (2017) is our target final mass.

Besides the mass values, Bond et al. (2017) determined the orbital parameters of the system, establishing that Sirius B orbits around the center of mass of the system in a 50.13 year period, with an eccentricity of 0.59. We have input these values in the calculations of our models.

Based on observations of stellar winds for Sirius A (Bertin et al. 1995), the mass loss rate derived from the MgII lines is between  $2 \times 10^{-13}$  and  $1.5 \times 10^{-12} M_{\odot}/\text{yr}$ . Factoring the broad range of ages derived from various stellar evolution models of 200 – 250 Myr (Bond et al. 2017; Liebert et al. 2005), the total mass loss for Sirius A is significantly smaller than the uncertainties in mass determinations from astrometry. For these reasons, we have decided to use a fixed mass of  $2.06 M_{\odot}$  for Sirius A, in our model grid.

One of the goals of our study is to better constrain the initial mass of Sirius B. Cummings et al. (2018) derived the IFMR based on self-consistent analysis of Sirius B and 79 white dwarfs from 13 clusters. Based on that study, and also considering previous IFMR studies, there is a rather large uncertainty in constraining the initial value masses. The current mass of Sirius B is  $1.018 \pm 0.011 M_{\odot}$ , which could have been from a progenitor with

initial mass from 4 to  $6.8 M_{\odot}$ . We have calculated our model grid with initial masses for Sirius B in that range, with  $0.1 M_{\odot}$  steps.

### 2.2. Photospheric parameters

With V magnitudes of -1.47 (Johnson & Morgan 1953) and 8.44 (Holberg et al. 1998) for Sirius A and B, respectively, therefore very distinct luminosities, this binary system imposed a puzzle for having comparable spectral energy distribution. The effective temperature of Sirius B is  $T_{\text{eff}} = 25193 \pm 37 \text{ K}$  (Barstow et al. 2005) and  $T_{\text{eff}} = 26083 \pm 378 \text{ K}$  (Bédard et al. 2017) from HST and ground-based optical spectroscopy respectively. We have used  $T_{\text{eff}}$  between 25000 and 26000 for Sirius B as a guide to establish the stopping condition of our calculated models. Bond et al. (2017) quotes the luminosity to be  $0.02448 \pm 0.00033 L_{\odot}$ , but using the Gaia magnitude  $G = 8.52$  and parallax  $\Pi = 374.49 \pm 0.23''$ , we calculated  $\log(L/L_{\odot}) = -1.54$ , by taking into account bolometric corrections.

Davis et al. (2011) used interferometry to determine the fundamental quantities of Sirius A. Through observations made at 694.1 nm, they determined the radius to be  $1.713 \pm 0.009 R_{\odot}$  by combining their measurements of the angular size with the Hipparcos parallax. They also determined the bolometric flux to be  $F = (5.32 \pm 0.14) \times 10^8 \text{ W/m}^2$ , the effective temperature and luminosity values yielded are  $T_{\text{eff}} = 9845 \pm 64 \text{ K}$  and  $L = 24.7 \pm 0.7 L_{\odot}$  respectively. We have used the luminosity and  $T_{\text{eff}}$  for Sirius A to constrain the initial metallicity of the system.

Petit et al. (2011) measured a constant, weak magnetic field of  $0.2 \pm 0.1 \text{ G}$  for Sirius A. Because there are no measurements of magnetic field for Sirius B, we have used this as the initial value for Sirius A and B. There is no evidence that both stars would have been born with different magnetic fields.

### 2.3. Metallicity

Payne (1925) made the first observational study of chemical abundances in stars, measuring the fraction of heavy elements in the universe. In principle, the abundance of any element other than helium can be compared to that of hydrogen to determine metallicity. The elemental abundance of a star can be used to empirically determine the age of the system, as younger stars will generally be more metal rich (Soderblom 2010). Metallicity can also provide insight as to how a star is evolving, as the isochrones of a population of stars and its evolutionary track can shift due to changes in its metal content (Bressan et al. 2012).

Modeling stellar evolution is dependent on the chemical abundance of the progenitor stars. For binary sys-

tems, we can assume that both stars have similar initial metallicities. Specifically for the Sirius system, since we cannot determine the original metallicity for Sirius B, we constrain its value based on the companion's on the main sequence, Sirius A (Qiu et al. 2021).

There have been multiple determinations of Sirius A's chemical abundances [e.g. (Cowley et al. 2016; Landstreet 2011)]. Regardless the scatter in the independent determinations and the analysis of different elements, all results point towards high metallicity values. However, previous attempts to model the stellar evolution of Sirius A cannot find high metallicity solutions compatible with the observed luminosity and the best fits for  $T_{\text{eff}}$ . Bond et al. (2017) computed evolutionary models using TYCHO and YREC codes and determined the best model to have a sub-solar metallicity of  $Z = 0.85 Z_{\odot}$ . It is important to note that the metallicity in the models is referred to as the initial value.

As an input in our models, we tested a broad range of metallicities, as the current values for Sirius A could have been somewhat contaminated by the planetary nebula of Sirius B.

#### 2.4. Past binary interaction

There are many reasons that support a lack of an interacting past, such as the rotation rate of Sirius A compared to other stars in its spectral class, their current separation, amongst others (Bond et al. 2017). Cowley et al. (2016) found evidence of copper and other heavy elements present in the spectra of Sirius A, indicating that there could have been accretion in the past due to the presence of s process elements. Bond et al. (2017) created a grid using TYCHO to determine if accretion influenced the evolution of Sirius A. They compiled models starting with a subsolar metallicity of  $0.9 Z_{\odot}$  and an initial mass of  $1.96 M_{\odot}$  and evolved the system until the AGB phase, right before pulsation, for 100 MYr (Bond et al. 2017). This, however, resulted in a radius that is too large for the current luminosity of Sirius A and an overall worse fit of the observed stellar parameters.

Based on the previous studies and observations, we have constructed our model grid assuming that the stars did not develop a common envelope nor that mass transfer happened in any stages of the past evolution of the system.

### 3. COMPUTATIONAL METHODS

MESA, or Modules for Experiments in Stellar Astrophysics, is an open-source code that allows users to model stellar structures and evolution (Paxton et al. 2011, 2013, 2015, 2018, 2019; Jermyn et al. 2023).

MESA uses numerical methods to simultaneously solve the coupled, non-linear differential equations for stellar evolution in a modular structure with a collection of Fortran libraries. MESA is used over a broad range of subjects, as it allows users the freedom in choosing prescriptions for various physical parameters (e.g. mass, wind, opacity, etc.). Besides single stars, MESA can be used to compute the evolution of binary systems.

We have used most recent release of MESA (version 23.05.1) to compute our model grid. We have used the binary capabilities of MESA (`evolve_both_stars` binary module) to model the Sirius system from the pre-main sequence up until the current observed evolutionary stage. MESA simultaneously evolves an interacting binary system, accounting for mass exchange, accretion, and changes to the orbital mechanics (Paxton et al. 2015).

Some of the assumptions this module makes is that the rotational axis is completely perpendicular to the orbital plane, which is a good enough approximation for most physical situations (Paxton et al. 2015). It can also account for the tidal interaction forces resulting from accretion, though this feature was not used in this analysis. The binary module is constructed with the Kolb and Ritter mass loss schemes, both of which are defined in Paxton et al. (2015).

The second module that we used was `make_co wd` to create a white dwarf with an even distribution of carbon and oxygen in the core, with a hydrogen and helium photosphere from a specified main sequence star (Jermyn et al. 2023). It is relevant to mention that this module omits the thermally pulsating phase (Jermyn et al. 2023).

### 4. MESA MODEL GRID

We computed stellar evolutionary models using MESA, evolving the binary system from the zero age main sequence until the current location of Sirius B in the white dwarf cooling sequence. As discussed in the previous sections, we have fixed the mass of Sirius A to be  $2.063 M_{\odot}$ . We have also fixed the value for magnetic field to be  $B = 0.2 \text{ G}$ . We have used the values for observed luminosities and best determinations of  $T_{\text{eff}}$  for Sirius A and B as guide for stopping conditions. This tells us that the metallicity values that make the model fit the spectroscopically observed parameters yield an accurate evolution. The MESA inlists and example models can be found via this [hyperlink](#).

#### 4.1. Testing Metallicity

As discussed in section 2.3, we assume that the original metallicity of Sirius B is the same as for Sirius A. We

started our calculations by using previous determinations of metallicity for Sirius A. We have computed evolutionary models in attempts to fit the observed metallicity of Sirius A.

In Figure 1, we plot our calculated evolutionary tracks of Sirius A for high (Sitnova et al. 2018), super-solar (Cowley et al. 2016), and solar metallicities compared to the observed luminosity and  $T_{\text{eff}}$ . None of our models are in agreement with the current observations of Sirius A. This discrepancy could be explained by the fact that the input values in the models are the initial metallicity and/or by possible contamination from the Sirius B planetary nebula.

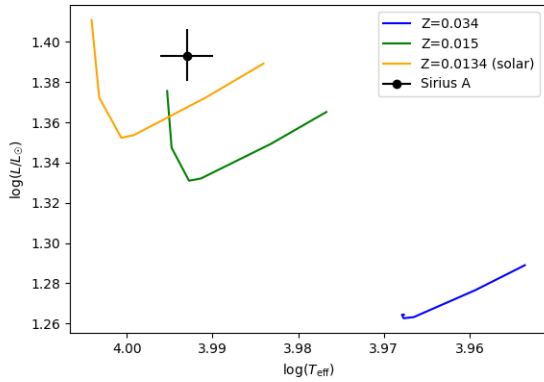


**Figure 1.** HR diagram for the evolutionary tracks of Sirius A for a high metallicity of  $[\text{Fe}/\text{H}] = 0.4$  (or  $Z = 0.034$ ) determined by Sitnova et al. (2018) (blue line), solar metallicity (orange line), and another model with super-solar of  $Z = 0.015$  estimated from Cowley et al. (2016) (green line), in comparison to the observed luminosity and  $T_{\text{eff}}$ . None of the high metallicity models is in agreement with the current position of Sirius A in the HR diagram.

We then proceeded to compute models with various metallicities from  $Z = 0.0115$  to  $0.0150$ , in steps of  $0.0005$ . In Figure 2, we plot evolutionary models for Sirius A, compared to the observed luminosity and measured  $T_{\text{eff}}$ . The best fit for initial metallicity of Sirius A is  $Z = 0.0124 \pm {}^{0.00073}_{0.00077}$ , a subsolar value ( $Z = 0.93 Z_{\odot}$ ), in agreement with previous calculations using TYCHO and YREC (Bond et al. 2017). We have used this value as the initial metallicity for both stars in the Sirius system.

#### 4.2. Mass of Sirius B

One of our main goals in computing evolutionary models is to better constrain the mass of the progenitor of Sirius B. We have varied the initial mass from  $4.0 M_{\odot}$  to  $6.8 M_{\odot}$ , in steps of  $0.1 M_{\odot}$ , using the luminosity, spectroscopic  $T_{\text{eff}}$ , and astrometric mass of Sirius B as a guide

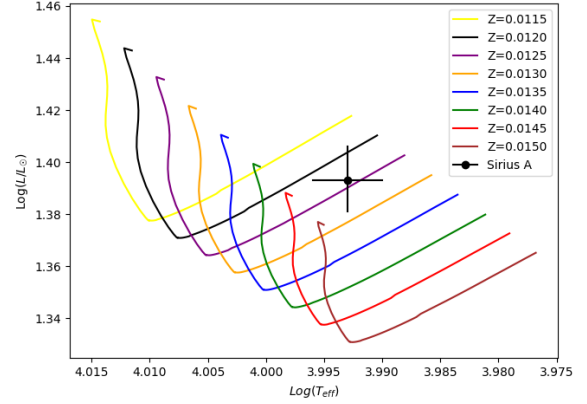


**Figure 2.** HR diagram for the evolutionary tracks calculated with MESA for Sirius A. We have used different initial metallicities from  $Z = 0.0115$  (yellow line, top left) to  $0.0150$  (dark red, bottom right), in steps of  $0.0005$ . Compared to the observed luminosity and determinations of  $T_{\text{eff}}$ , our best fit is a subsolar metallicity of  $Z = 0.0124 \pm {}^{0.00073}_{0.00077}$ .

for stopping condition, and implementing the best fit for the metallicity as an initial condition, from the analysis on Sirius A.

#### 4.3. Other parameters into the models

We computed our models with a mesh delta coefficient of  $3.75$ . This coefficient is related to how incrementally the code splits up the star. At each of the boundaries created by this mesh, the equations of stellar evolution are solved and made to be continuous across the boundary. Mass overflow was monitored by the Roche Lobe overflow limit, which determines if accretion would occur, making the binary stars interact in a significant manner. For the Sirius system, the orbital solution from astrometry places the stars too far apart for mass transfer.

We modeled the progenitor of Sirius B taking into account wind mass loss effects. We selected the MESA's wind mass loss function that computes stellar angular momentum while taking into account the removed layers' momentum (Paxton et al. 2011).

### 5. RESULTS

We have computed evolutionary models for both stars simultaneously, assuming that the initial mass for Sirius A as  $M = 2.063 M_{\odot}$ , non-interacting stars, and neglecting mass loss for Sirius A. In Table 1, we summarize the initial parameters of our model grid.

In Table 2, we list the values of our model grid calculations for Sirius B: initial and final masses, age, and  $T_{\text{eff}}$ . The metallicities used for the analysis of Sirius B were based on the values for Sirius A that best fit the

	$M (M_{\odot})$	$Z$	$\log L/L_{\odot}$	$\log T_{\text{eff}}$	$B \text{ (G)}$
A	2.063	0.0124	1.37 – 1.39	3.993 – 4.001	0.2
B	4 – <b>6.8</b>	0.0124	-1.62 – -1.54	4.398 – 4.433	0.2

**Table 1.** Fundamental stellar parameters used to calculate models with MESA `evolve_both_stars`. We assumed that there was no mass transfer between the two stars and that the mass of Sirius A stays constant throughout its time on the main sequence, because of the negligible mass loss. This temperature range and luminosity were used to place stopping conditions in the evolutionary models.

observed luminosity and spectroscopic  $T_{\text{eff}}$ , in the range  $Z = 0.0124 \pm_{0.00077}^{0.00073}$ .

$M_{\text{initial}} (M_{\odot})$	$M_{\text{final}} (M_{\odot})$	Age ( $10^8$ years)	$\log(T_{\text{eff}})$
4.0	0.839	3.006	4.369
4.1	0.855	2.905	4.367
4.2	0.861	2.803	4.372
4.3	0.869	2.714	4.375
4.4	0.873	2.663	4.377
4.5	0.880	2.550	4.379
4.6	0.889	2.483	4.381
4.7	0.900	2.430	4.376
4.8	0.888	2.372	4.379
4.9	0.894	2.322	4.381
5.0	0.901	2.275	4.390
5.1	0.907	2.227	4.385
5.2	0.914	2.198	4.396
5.3	0.949	2.169	4.401
5.4	0.930	2.139	4.401
5.5	0.970	2.121	4.406
5.6	0.945	2.071	4.409
5.7	0.955	2.050	4.415
5.8	0.964	2.016	4.411
5.9	1.039	1.834	4.443
6.0	1.015	2.036	4.414
6.1	1.047	2.114	4.420
6.2	1.038	2.008	4.424
6.3	1.092	1.882	4.444
6.4	1.115	2.138	4.442
6.5	1.142	2.187	4.459
6.6	1.147	1.939	4.467
6.7	1.155	1.989	4.459
6.8	1.168	2.146	4.468

**Table 2.** Table of models calculated for Sirius B at the metallicity of  $Z = 0.0124$ , for different initial and final masses, ages, and  $T_{\text{eff}}$ .

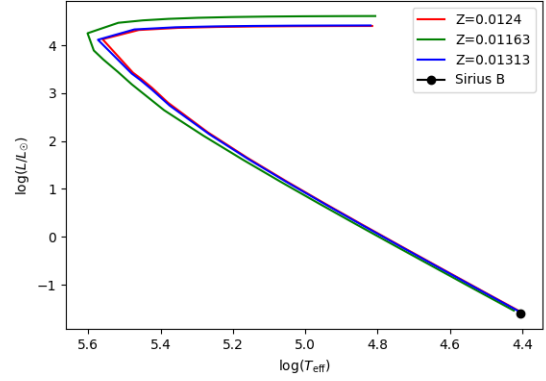


**Figure 3.** HR Diagram for Sirius B for the best fit metallicity, including the upper and lower bounds, for a progenitor mass of  $6.0 M_{\odot}$ . The white dwarf cooling track agrees with the current placement of Sirius B on the luminosity temperature plane.

In Figure 3, we plot the HR diagrams showing models for the white dwarf cooling sequence, for a fixed progenitor mass of  $6.0 M_{\odot}$ , for the upper and lower limits in metallicity, determined from Sirius A. For white dwarf cooling, changes in metallicity produce minute changes in the evolutionary tracks.

Once the models were calculated, we searched in our grid for the solutions closest to the mass ( $M$ ) from astrometry (Bond et al. 2017), effective temperature ( $T_{\text{eff}}$ ) from spectroscopy (Barstow et al. 2005; Bédard et al. 2017), and luminosity ( $L$ ) from astrometry and parallax (Bond et al. 2017). We minimized the squared of the differences of the normalized physical quantities ( $\xi_i$ ) listed above ( $M$ ,  $T_{\text{eff}}$ ,  $L$ ) from the models and the observations as:

$$\chi = \sqrt{\sum_i \left( \frac{\xi_{i,\text{observed}} - \xi_{i,\text{model}}}{\xi_{i,\text{observed}}} \right)^2} \quad (1)$$

In Fig. 4, we plot our models and the minimized observed quantities of  $T_{\text{eff}}$  and luminosity. We also use mass as a third constraint to put limits on viable models. Fig. 5 and Fig. 6 display the other views of this three-dimensional space. Our best solution for initial mass of Sirius B and the age of the system are  $6.0 M_{\odot}$  and 203.6 Myr, respectively. By using the uncertainties in luminosity, spectroscopic  $T_{\text{eff}}$  and astrometric mass, we computed that the uncertainties in the age of the system is  $\pm 45$  Myr, and in progenitor mass for Sirius B is  $\pm 0.6 M_{\odot}$ . Additionally, our models indicated an  $T_{\text{eff}} = 25882 \pm 2332$  K for Sirius B.

## 6. COMPARISON TO PREVIOUS DETERMINATIONS



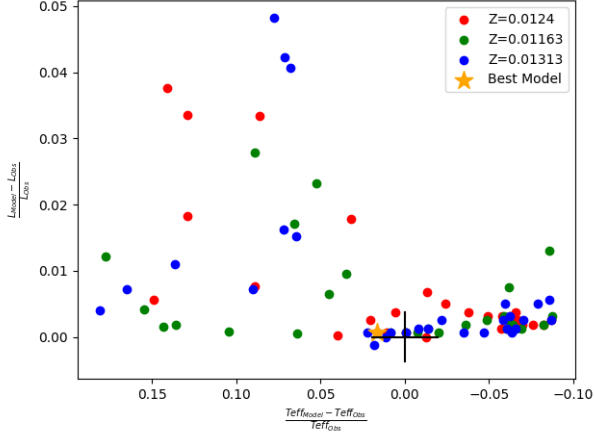


**Figure 4.** Comparison between models and the observations of Sirius B in  $L$ - $T_{\text{eff}}$  plane. The best model (yellow star) was found by the minimization of the normalized luminosity, spectroscopic  $T_{\text{eff}}$ , and astrometric mass (not displayed in this plot). The models are for the calculated metallicity (red dots) and upper and lower limits (blue and green dots, respectively). The spread of the models becomes large for progenitor masses over  $6.2 M_{\odot}$ .

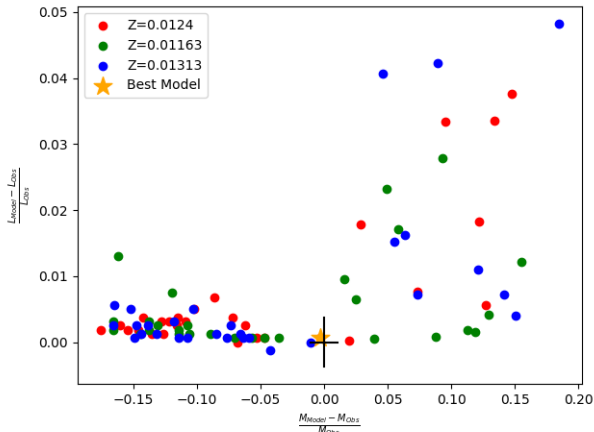


**Figure 5.** Comparison between models and the observations of Sirius B in  $L$ - $M$  plane. Just as before, The best model (yellow star) was found by the minimization of the normalized luminosity, spectroscopic  $T_{\text{eff}}$ , and astrometric mass. This plot highlights that smaller initial masses of Sirius B do not fit the spectroscopic parameters very well. With this, we can put a lower limit on acceptable progenitor masses.

We now turn to review how our determinations compare with results from previous studies.

In addition to the orbital solution and mass determinations for the Sirius system, Bond et al. (2017) modelled the evolution of the stars, using the “Montreal” photometric tables for white dwarf cooling sequences (Holberg & Bergeron 2006), combined with PARSEC

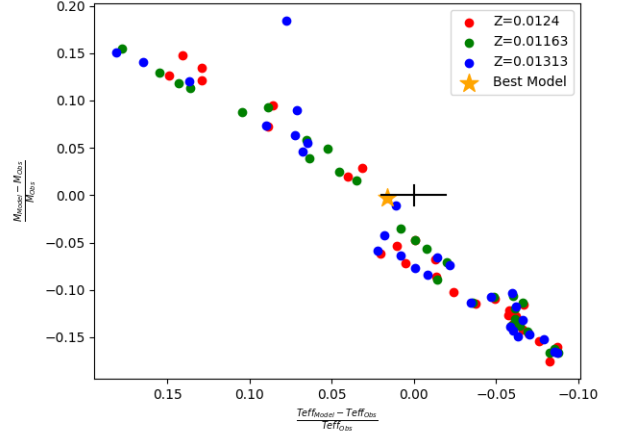


**Figure 6.** Comparison between models and the observations of Sirius B in  $M$ - $T_{\text{eff}}$  plane. Despite there being many models that fall into the range of acceptable temperature, the mass is so well constrained that it limits the possible solutions.

(Bressan et al. 2012) and YREC evolutionary models (Demarque et al. 2008). They have determined the total age of Sirius B is  $228 \pm 10$  Myr, for a cooling age of  $\sim 126$  Myr. For Sirius A, using a slightly subsolar metallicity of about  $0.85 Z_{\odot}$ , they found that the best models yield ages between 237 and 247 Myr, with uncertainties of  $\pm 15$  Myr, consistent with that of the white dwarf companion. In a previous study, Liebert et al. (2005) using similar model grids determined the age of Sirius system to be 225–250 Myr. Our best solution for age is  $203.6 \pm 45$  Myr, which within  $2\sigma$  from the other determinations, or 10% difference.

This discrepancy in age determination can be explained from different prescription in the physics and choices in physical quantities input in the models. Obviously, mass is the most important parameter, which dictates stellar evolution. Bond et al. (2017) estimated the progenitor mass for Sirius B to be  $5.6 \pm 0.6 M_{\odot}$  from PARSEC, and  $5.0 \pm 0.2 M_{\odot}$  from YREC models. Our models fit best a progenitor with  $6.0 \pm 0.6 M_{\odot}$ , which makes the Sirius system younger than previously determined. From our Table 2, the 225 Myr model would be for the a star with an initial mass of  $5.05 M_{\odot}$ , consistent with the previous determinations. However, the final mass is  $0.904 M_{\odot}$ , which is smaller than the astrometric mass and off by  $10\sigma$ . Since the final mass of Sirius B is one of the most reliable measurements for this system, we can state that using different evolutionary codes will yield external uncertainties of about 20 Myr in age,  $1 M_{\odot}$  in initial mass, and  $0.1 M_{\odot}$  in final mass.

Metallicity also affects the evolutionary timescales in the models, as stars with higher percentage of metals have a shorter lifetime. Bond et al. (2017) used in

their evolutionary model calculations a metallicity of  $Z = 0.85 Z_{\odot}$ , while our best fit is for  $Z = 0.92_{0.05}^{0.06} Z_{\odot}$ , both subsolar values. Because our determination is for a larger metallicity, our age determination, as expected, is a younger system.

Finally, one of our main goals with this study is to contribute in constraining of the IFMR. Cummings et al. (2018) determined the IFMR by creating isochrones for a dataset of clusters and binary stars using PARSEC and MIST non-rotating isochrones.

However due to the large initial mass of our solution, the IFMR is smaller in comparison to the PARSEC and MIST determinations with a value of  $0.169 M_{\text{final}}/M_{\text{initial}}$  versus  $0.177 M_{\text{final}}/M_{\text{initial}}$  for a  $6.0 M_{\odot}$  progenitor (Cummings et al. 2018).

Our best fit for the initial and final mass for Sirius B contributes into the spread in determinations, due to the higher metallicity.

## 7. CONCLUSION AND FUTURE WORKS

In this paper, we report our best fit solutions to model the Sirius system, by using MESA models, constraining the parameter space with the observational physical quantities. We discussed our levels of confidence and the reasoning of why some quantities place stronger constraints than others. Our best model for metallicity of Sirius A is  $Z = 0.0124$ , and using a fixed mass of  $2.063 M_{\odot}$  from astrometry and Sirius B’s luminosity,  $T_{\text{eff}}$ , and final mass, yields a progenitor mass of  $6.0 \pm 0.6 M_{\odot}$ . This is in agreement with Bond et al. (2017), the main differences being our larger progenitor mass for Sirius B and the notably lower age of the

system. Using the PARSEC and Tycho IFMR’s, Bond et al. (2017) obtained initial masses of  $5.6 \pm 0.6 M_{\odot}$  and  $5.0 \pm 0.2 M_{\odot}$ . Our results fall into the range of the PARSEC model, but the values determined with the YREC code are significantly smaller, in part due to the lower metallicity chosen by Bond et al. (2017) and possibly also the treatment of the thermal pulsations during the ABG phase.

We have used a non-interactive model for the Sirius system, based on the current orbital solution from previous studies. The fact that we could not fit the current observed high metallicity for Sirius A remains a puzzle, but we argue that the state-of-the-art models only take into account substantial interactions between binary stars and cannot account for minor pollution from the planetary nebula.

There are limitations in our calculations due to assumptions and choices in parameters for the calculations of the models. We must point out that we have not changed the time step nor the mesh point between each model. However, we have presented a systematic approach to modeling evolution of binary systems, constraining the most reliable physical parameters, while varying the least precise ones within the uncertainties. We have also discussed the external uncertainties between our determinations and the ones from previous studies. We are encouraged by our results to expand the parameter space in our calculations since our results are consistent with the ones derived using other model grids. We will then attempt to model other binary systems, starting with “Sirius-like” systems and expanding into interacting systems.

## REFERENCES

- Adams, W. S. 1915, PASP, 27, 236, doi: [10.1086/122440](https://doi.org/10.1086/122440)
- Barstow, M. A., Bond, H. E., Holberg, J. B., et al. 2005, MNRAS, 362, 1134, doi: [10.1111/j.1365-2966.2005.09359.x](https://doi.org/10.1111/j.1365-2966.2005.09359.x)
- Bédard, A., Bergeron, P., & Fontaine, G. 2017, ApJ, 848, 11, doi: [10.3847/1538-4357/aa8bb6](https://doi.org/10.3847/1538-4357/aa8bb6)
- Bertin, P., Lamers, H. J. G. L. M., Vidal-Madjar, A., Ferlet, R., & Lallement, R. 1995, A&A, 302, 899
- Bessel, F. W. 1844, MNRAS, 6, 136, doi: [10.1093/mnras/6.11.136](https://doi.org/10.1093/mnras/6.11.136)
- Bond, H. E., Schaefer, G. H., Gilliland, R. L., et al. 2017, ApJ, 840, 70, doi: [10.3847/1538-4357/aa6af8](https://doi.org/10.3847/1538-4357/aa6af8)
- Bressan, A., Marigo, P., Girardi, L., et al. 2012, MNRAS, 427, 127, doi: [10.1111/j.1365-2966.2012.21948.x](https://doi.org/10.1111/j.1365-2966.2012.21948.x)
- Cowley, C. R., Ayres, T. R., Castelli, F., et al. 2016, ApJ, 826, 158, doi: [10.3847/0004-637X/826/2/158](https://doi.org/10.3847/0004-637X/826/2/158)
- Cummings, J. D., Kalirai, J. S., Tremblay, P. E., Ramirez-Ruiz, E., & Choi, J. 2018, ApJ, 866, 21, doi: [10.3847/1538-4357/aadfd6](https://doi.org/10.3847/1538-4357/aadfd6)
- Davis, J., Ireland, M. J., North, J. R., et al. 2011, PASA, 28, 58, doi: [10.1071/AS10010](https://doi.org/10.1071/AS10010)
- Demarque, P., Guenther, D. B., Li, L. H., Mazumdar, A., & Straka, C. W. 2008, Ap&SS, 316, 31, doi: [10.1007/s10509-007-9698-y](https://doi.org/10.1007/s10509-007-9698-y)
- Holberg, J. B., Barstow, M. A., Bruhweiler, F. C., Cruise, A. M., & Penny, A. J. 1998, ApJ, 497, 935, doi: [10.1086/305489](https://doi.org/10.1086/305489)
- Holberg, J. B., & Bergeron, P. 2006, AJ, 132, 1221, doi: [10.1086/505938](https://doi.org/10.1086/505938)
- Holberg, J. B., Oswalt, T. D., Sion, E. M., Barstow, M. A., & Burleigh, M. R. 2013, MNRAS, 435, 2077, doi: [10.1093/mnras/stt1433](https://doi.org/10.1093/mnras/stt1433)

- Jermyn, A. S., Bauer, E. B., Schwab, J., et al. 2023, ApJS, 265, 15, doi: [10.3847/1538-4365/aca8d](https://doi.org/10.3847/1538-4365/aca8d)
- Johnson, H. L., & Morgan, W. W. 1953, ApJ, 117, 313, doi: [10.1086/145697](https://doi.org/10.1086/145697)
- Landstreet, J. D. 2011, A&A, 528, A132, doi: [10.1051/0004-6361/201016259](https://doi.org/10.1051/0004-6361/201016259)
- Liebert, J., Young, P. A., Arnett, D., Holberg, J. B., & Williams, K. A. 2005, ApJL, 630, L69, doi: [10.1086/462419](https://doi.org/10.1086/462419)
- Luyten, W. J. 1922, PASP, 34, 356, doi: [10.1086/123249](https://doi.org/10.1086/123249)
- Paxton, B., Bildsten, L., Dotter, A., et al. 2011, ApJS, 192, 3, doi: [10.1088/0067-0049/192/1/3](https://doi.org/10.1088/0067-0049/192/1/3)
- Paxton, B., Cantiello, M., Arras, P., et al. 2013, ApJS, 208, 4, doi: [10.1088/0067-0049/208/1/4](https://doi.org/10.1088/0067-0049/208/1/4)
- Paxton, B., Marchant, P., Schwab, J., et al. 2015, ApJS, 220, 15, doi: [10.1088/0067-0049/220/1/15](https://doi.org/10.1088/0067-0049/220/1/15)
- Paxton, B., Schwab, J., Bauer, E. B., et al. 2018, ApJS, 234, 34, doi: [10.3847/1538-4365/aaa5a8](https://doi.org/10.3847/1538-4365/aaa5a8)
- Paxton, B., Smolec, R., Schwab, J., et al. 2019, ApJS, 243, 10, doi: [10.3847/1538-4365/ab2241](https://doi.org/10.3847/1538-4365/ab2241)
- Payne, C. H. 1925, PhD thesis, RADCLIFFE COLLEGE.
- Petit, P., Lignières, F., Aurière, M., et al. 2011, A&A, 532, L13, doi: [10.1051/0004-6361/201117573](https://doi.org/10.1051/0004-6361/201117573)
- Qiu, D., Tian, H.-J., Wang, X.-D., et al. 2021, ApJS, 253, 58, doi: [10.3847/1538-4365/abe468](https://doi.org/10.3847/1538-4365/abe468)
- Russell, H. N. 1944, AJ, 51, 13, doi: [10.1086/105780](https://doi.org/10.1086/105780)
- Sitnova, T. M., Mashonkina, L. I., & Ryabchikova, T. A. 2018, MNRAS, 477, 3343, doi: [10.1093/mnras/sty810](https://doi.org/10.1093/mnras/sty810)
- Soderblom, D. R. 2010, ARA&A, 48, 581, doi: [10.1146/annurev-astro-081309-130806](https://doi.org/10.1146/annurev-astro-081309-130806)
- van Leeuwen, F. 2007, A&A, 474, 653, doi: [10.1051/0004-6361:20078357](https://doi.org/10.1051/0004-6361:20078357)